Suppression of Dripping from a Ceiling

John M. Burgess,* Anne Juel,† W. D. McCormick, J. B. Swift, and Harry L. Swinney‡
Center for Nonlinear Dynamics and Department of Physics, The University of Texas at Austin, Austin, Texas 78712
(Received 18 July 2000)

An isothermal layer suspended from a surface is gravitationally (Rayleigh-Taylor) unstable. We find that, when a vertical temperature difference ΔT above a critical value $(\Delta T)_c$ is imposed across the liquid-gas layer system (heated from below), the restoring force provided by the temperature-dependent surface tension (thermocapillarity) can stabilize the layer. Our measurements of the most unstable wave number for $\Delta T < (\Delta T)_c$ agree well with our linear stability analysis. The instability occurs at long wavelengths: the most unstable wavelength at $(\Delta T)_c$ is infinite.

DOI: 10.1103/PhysRevLett.86.1203 PACS numbers: 47.20.Dr, 47.20.Ma, 68.15.+e

A layer of water suspended from a ceiling will drip, as anyone with a leaky roof can attest. In general, any thin liquid coating applied to the underside of a surface will drip. That is, the interface between a liquid layer above a gas layer is unstable to infinitesimal deformations, as shown in the classic works of Rayleigh, Taylor, and Lewis [1]. Suppression of this *Rayleigh-Taylor* instability was demonstrated by applying vertical oscillations [2] and was predicted for applied electric fields [3] and temperature gradients [4]. In our paper, we demonstrate that the Rayleigh-Taylor instability can be suppressed with a vertical temperature gradient.

A perturbation of the depth of the liquid layer produces thicker regions where the interface becomes warmer and thinner regions where it becomes colder. Since the surface tension decreases with temperature, fluid is pulled along the interface from the warmer regions of lower surface tension toward the colder regions of higher surface tension, as indicated in Fig. 1(a). Thus thermocapillary stresses act to stabilize the liquid layer [4].

Our experiments examine the stability of a silicone oil layer of thickness d (0.0125 cm) suspended above a gas layer of thickness d_g (0.0275 cm) with an imposed temperature on the lower boundary hotter than the temperature of the upper boundary [see Fig. 1(a)]. Properties of the fluids are given in [5]. We will first describe our analysis and experimental methods and then will present a comparison of experiment and theory.

Our analysis uses a modified form of an evolution equation obtained by VanHook *et al.* [6], who studied the stably stratified problem of a gas layer *above* a liquid layer; in that case thermocapillarity is destabilizing and gravity is stabilizing, while in our case thermocapillarity is stabilizing and gravity is destabilizing. With a change of sign of the temperature gradient and gravitational acceleration terms, the evolution equation for the liquid depth h from [6] applies to our thin-film Rayleigh-Taylor instability:

$$\frac{\partial h}{\partial t} = \nabla \cdot \left\{ \frac{M}{2} \frac{Q h^2 \nabla h}{(Q - Fh)^2} - \frac{G}{3} h^3 \nabla h - \frac{S}{3} h^3 \nabla^2 \nabla h \right\}, \quad (1)$$

where the three terms in the brackets describe thermocapillary, gravitational, and surface tension effects, respectively. The Marangoni number for the liquid layer is $M = (d\sigma_T \Delta T/\rho\nu\kappa)(1 + d_g k/dk_g)^{-1}$, the Galileo number is $G = gd^3/\nu\kappa$, the inverse crispation number is $S = \sigma d/\rho\nu\kappa$, the two-layer Biot number is $F = (k/k_g - 1)(1 + d_g k/dk_g)^{-1}$, $Q = 1 + F$. The thickness and thermal conductivity of the liquid (gas) layer, respectively, are d (d_g) and k (k_g), and the temperature difference imposed across the liquid-gas system is ΔT [7]. The temperature coefficient of surface tension is $\sigma_T \equiv -d\sigma/dT$; ρ, ν, and κ are the liquid density, kinematic viscosity, and thermal diffusivity, respectively. Time has been nondimensionalized by d^2/κ and length by d.

A linear stability analysis of (1) about a flat interface with periodic boundary conditions yields a stable layer for $\Delta T > (\Delta T)_c$, where

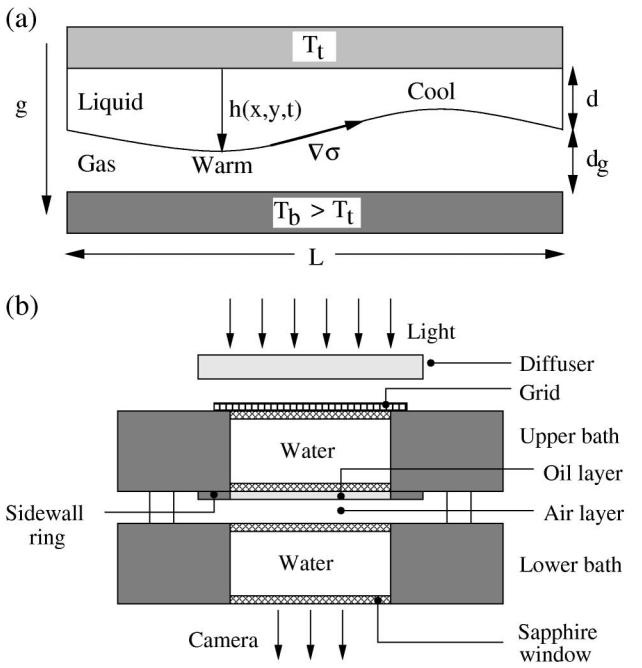

FIG. 1. (a) Suspended liquid layer geometry with an imposed temperature difference $\Delta T = T_b - T_t > 0$. (b) Schematic of the apparatus.

 © 2001 The American Physical Society

$$(\Delta T)_c = \frac{2}{3}\frac{\rho g d^2}{\sigma_T}\frac{(1 + d_g k/dk_g)^2}{(k/k_g)(1 + d_g/d)}. \quad (2)$$

The (dimensionless) growth rate is

$$\gamma(q) = \frac{G}{3} q^2\left[\epsilon - \left(\frac{q}{q_{\rm cap}}\right)^2\right], \quad (3)$$

where $\epsilon = [(\Delta T)_c - \Delta T]/(\Delta T)_c$ is the reduced temperature, q is the wave number of the perturbation, and $q_{\rm cap} = \sqrt{\rho g d^2/\sigma}$ is the (dimensionless) capillary wave number. The predicted growth rate dependence on wave number and temperature is shown in Fig. 2 for the conditions of our experiment [5].

For $\Delta T < (\Delta T)_c$, the analysis predicts that the wave number of the mode with the maximum growth rate is

$$q^* = q_{\rm cap}\sqrt{\epsilon/2}, \quad (4)$$

and that modes are unstable up to a maximum wave number, $q_{\rm max} = \sqrt{2}\, q^*$; perturbations to the height of the interface with $q > q_{\rm max}$ will have negative growth rates. This is a long wavelength instability: The wave number q^* of the most unstable mode goes to zero as $(\Delta T)_c$ is approached.

Our oil-air layer system is sandwiched between two sapphire windows (5.0 cm in diameter), each of which is in contact with a temperature-controlled circulating water bath [see Fig. 1(b)]. ΔT is controlled to ± 0.05 K, which is small compared to the typical ΔT, 10 K. The windows are adjusted interferometrically, parallel and level to $(1.2 \pm 0.1) \times 10^{-4}$ rad. The thickness of the oil layer, $d = 0.0125 \pm 0.0003$ cm, is set by the height of a brass sidewall ring that encircles the oil layer; the horizontal surface of the ring is treated with a nonwetting agent.

The oil layer is prepared by first inverting the window encircled by the brass sidewall and then applying the oil using a microliter glass syringe. The viscous oil (200 cS) spreads slowly over the window and pins at the corner of the sidewall. After several hours, this window is reinverted to obtain a suspended oil layer, as shown in Fig. 1(b).

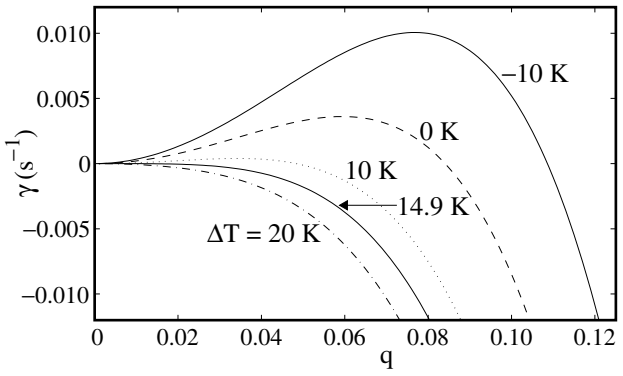

FIG. 2. Predicted growth rate γ [(3) dimensionalized by d^2/κ] as a function of the dimensionless wave number q for several applied temperature differences ΔT. For $\Delta T > 14.9$ K, the layer is predicted to be stable for all wave numbers.

The oil-air layer interface position is visualized using deflectometry, in which the oil layer serves as a variable-thickness lens [8]. A fine grid is imaged through the oil layer using a CCD camera interfaced to a computer. The grid, a thin transparent plastic sheet with square transparent spaces (0.018 cm wide) between the grid lines (0.036 cm), is placed directly on the upper bath top window. Light passing through the oil layer is refracted at the oil-air interface, distorting the image of the grid as the interface deforms. The displacement of an imaged grid point (in units of d) is $\delta = \beta(n_{\rm air} - n_{\rm oil})(2d_s/n_s + d_w/n_w)$, where $|\beta| \ll 1$ is the local slope of the interface; $n_{\rm air} = 1$, $n_{\rm oil} = 1.41$, $n_s = 1.77$, and $n_w = 1.33$ are the indices of refraction for air, oil, sapphire, and water, respectively, and $d_s = 0.3175$ cm and $d_w = 2.54$ cm are the thickness of each sapphire window and the water between the windows in each bath, respectively. Then, with δ in units of pixels in the image, we have $\beta \approx 0.008\delta$. The minimum slope we can detect is about 0.3°; thus a mode with a half-wavelength equal to the width of the layer must have an amplitude comparable to the layer depth to be detectable.

The formation of a drop is illustrated in Fig. 3. The cumulative displacement vectors for the grid points in the images [Fig. 3(a)] are shown in Fig. 3(b); the vector slope of the interface is calculated at each grid point; numerical integration then yields the surface height [Fig. 3(c)].

Measurements of the most unstable wave number as a function of ΔT are compared with our linear stability analysis in Fig. 4. Theory and experiment agree well. To obtain each data point, we set $\Delta T < (\Delta T)_c$, inverted the oil layer, and observed the emergence of deformations using the technique described above. We determine the most unstable wave number by scaling the average width of a reconstructed drop at half its maximum height by 3, since the width at half the maximum height of a sinusoidal deformation is one-third of the full wavelength. We determine the wave number by this method since Fourier analysis is inappropriate for a long wavelength instability, where the wavelength is comparable to the width of the system. Far below the onset of instability the wave number would be large enough so that many drops would form, producing more regular patterns if the air layer were sufficiently thick, as has been observed for an isothermal suspended layer [8].

The growth rate of the most unstable wave number predicted by linear analysis assumes exponential time dependence of the most unstable mode in the perturbation. We examine this point by setting $\Delta T < (\Delta T)_c$ and then inverting the oil layer. We then observe an initial exponential increase in the depth of a drop, as Fig. 5(a) illustrates. At longer times there is a transition to a constant growth rate; this change in behavior is likely due to an increase in nonlinear effects as the drop grows larger. Comparison of theory and experiment for the regime with exponential growth is shown in Fig. 5(b). The data exhibit a decrease in growth rate with increasing ΔT as

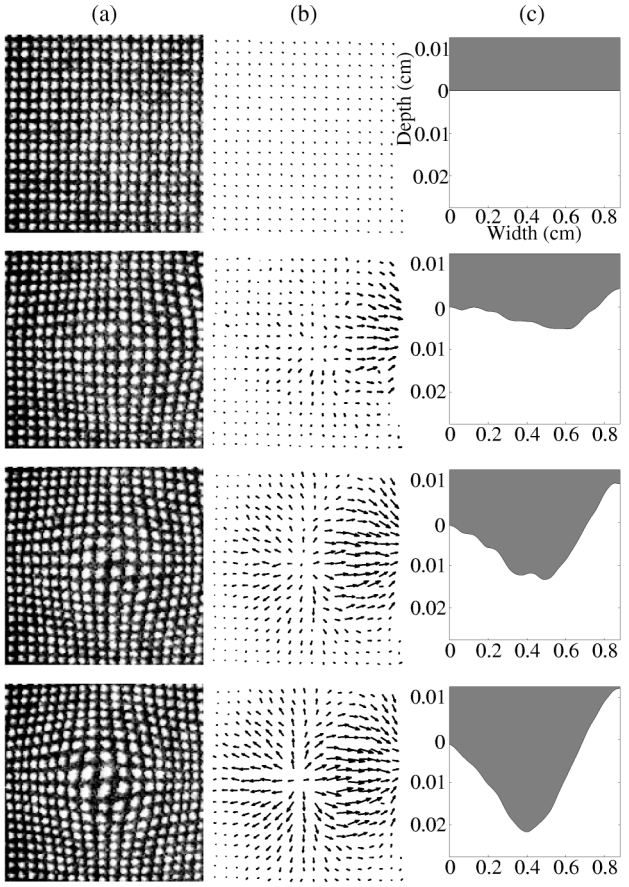

FIG. 3. Drop formation: (a) A sequence of grid images (at $t = 0$, 720, 760, and 800 s) illustrating the formation of an isothermal drop. The width of the region shown is 1.2 cm. (b) The accumulated vector displacement field of the grid points. (c) A cross section through the center of the reconstructed drop (the ordinate zero is at the original position of the interface); the surface ripples arise from sparse sampling of the image, while the asymmetry is due to the formation of a nearby drop. In (c) the vertical scale is expanded 25 times compared to the horizontal scale.

predicted, but the uncertainty in the data is large because the exponential regime is observable over only a small fraction of an e-folding time.

The observed decrease in the drop growth rate toward zero with increasing ΔT [Fig. 5(b)] suggests that it should be possible to stabilize the gravitationally unstable oil layer with a sufficiently large ΔT. Indeed, we find that suspended layers can be stabilized and, once stabilized, they can be maintained indefinitely—some layers have been maintained stable for more than a week. However, most of our attempts to obtain a stable inverted layer were not successful because the process of producing a suspended layer by inverting an upward-facing layer inevitably produced a large amplitude perturbation at the longest possible wavelength, which is the most unstable mode: If the window is inverted slowly, the layer is thicker at its lower end and a drop forms there, while, if the window is inverted rapidly, the layer is thicker at the upper end and a drop forms there.

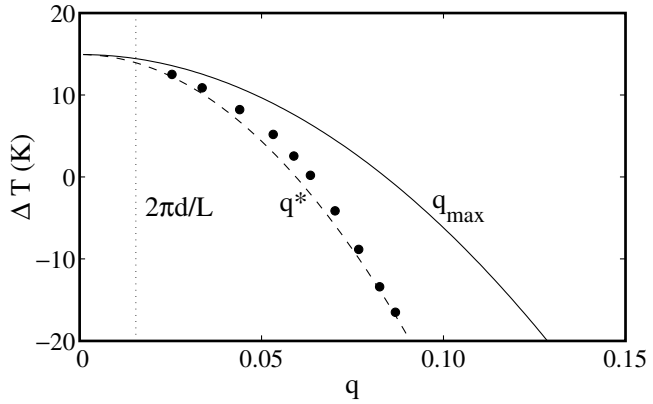

FIG. 4. Measurements (•) of the most unstable wave number q^* compared with the prediction of a linear stability analysis (dashed curve). The solid curve corresponds to the maximum unstable wave number (see text). The measurements are made immediately before a drop touches the bottom boundary; the maximum deformation of a drop is typically only 1% of the measured wavelength. The vertical dotted line shows the value of q corresponding to the diameter of the experimental system. The uncertainties in q are approximately equal to the size of a data point in the plot. Negative ΔT corresponds to the top boundary hotter than the bottom boundary.

Nevertheless, with ΔT set a few degrees above critical, we were able to produce stable layers about 10% of the time.

The lower limit of stability of stabilized layers was determined by decreasing ΔT in small steps, starting with

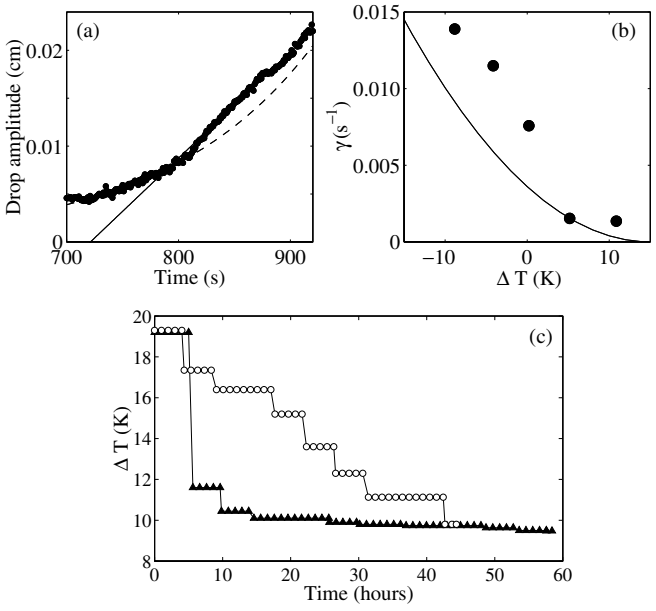

FIG. 5. Drop growth: (a) The drop size grows exponentially (dashed curve) at early times and linearly (solid line) at later times. (b) Predicted $\gamma(q^*)$ (solid curve) and measured drop growth rate (•). In (a) and (b), as in Fig. 4, we set $\Delta T < (\Delta T)_c$ before inversion of the layer. (c) Two experimental determinations of the loss of stability of a liquid layer initially stabilized at $\Delta T = 19.3$ K [$\Delta T > (\Delta T)_c$]. The temperature was decreased at different rates, but in both cases the drop formed at 9.7 ± 0.2 K.

a layer that had been stabilized for approximately 4 h. The results were reproducible for a wide range of temperature histories, as Fig. 5(c) illustrates for two cases. The ΔT at which the layer became unstable, 9.7 K, was lower than that given by (2), 14.9 K [9], perhaps because, after an inverted layer had relaxed to form a flat layer, the pinned edge of the layer suppressed the most unstable (long wavelength) mode. We measured the instability for three air layer depths [including $d_g = 0.0275$ cm corresponding to Figs. 4 and 5(c)] and found that the difference between the observed ΔT at onset and the predicted value changes sign at $F \approx 1/2$. For $d_g = 0.0275$ cm ($F = 0.35$), 0.0206 cm ($F = 0.45$), and 0.0138 cm ($F = 0.65$), the observed ΔT at onset was 30% below, 10% below, and 30% above the predicted value, respectively. In a study of the stably stratified case [10], a dependence of onset on initial interface profile was found to be minimal for small $|F - 1/2|$ and stronger for large $|F - 1/2|$. The pinning condition was found to be crucial in determining the non-uniform base interface shape in [10]. Therefore, we conjecture that pinning of the liquid layer at the sidewall is a source of the deviation from the predictions of linear analysis we observe. We emphasize that the data in Figs. 4 and 5(c) were obtained under different protocols: for Fig. 4 and Figs. 5(a) and 5(b) we set $\Delta T < (\Delta T)_c$ and then the oil layer was inverted, while for Fig. 5(c) we set $\Delta T > (\Delta T)_c$ before inversion. This difference, together with the pinning, may be the source of the difference between the $(\Delta T)_c$ measured in Fig. 5(c) and the data in Fig. 4.

In summary, we have demonstrated thermocapillary stabilization of a Rayleigh-Taylor unstable interface. Future experiments could use interferometry to detect the growth of the most unstable (long wavelength) mode, which is not observable in our deflectometry measurements. Future experiments should also examine the effect of boundary conditions by varying the wetting properties and geometry of the sidewalls and by examining larger width layers and various liquid layer depths. Such measurements together with linear and nonlinear analyses of the evolution equation (1) including realistic boundary conditions with sidewall pinning in a finite (rather than infinite) width layer should provide a better understanding of thermocapillary stabilization of Rayleigh-Taylor unstable layers.

We thank S. VanHook, D. Goldman, M. Shattuck, P. Matthews, and E. Knobloch for helpful discussions. This work was supported by the Office of Naval Research and by NASA Grants No. NAG3-1839 and No. NCCS5-154.

*Electronic address: jburgess@chaos.ph.utexas.edu
†Present address: Department of Physics and Astronomy, University of Manchester, Manchester M13 9PL, United Kingdom.
‡Electronic address: swinney@chaos.ph.utexas.edu

[1] Lord Rayleigh, *Scientific Papers* (Cambridge University Press, Cambridge, England, 1900), Vol. II; G. I. Taylor, Proc. R. Soc. London A **201**, 192 (1950); D. J. Lewis, Proc. R. Soc. London A **202**, 81 (1950).

[2] G. H. Wolf, Phys. Rev. Lett. **24**, 444 (1970).

[3] N. A. Bezdenezhnykh, V. A. Briskman, A. A. Cherepanov, and M. T. Sharov, Fluid Mech. Sov. Res. **15**, 11 (1986).

[4] B. K. Kopbosynov and V. V. Pukhnachev [Fluid Mech. Sov. Res. **15**, 95 (1986)] predicted thermocapillary stabilization of a Rayleigh-Taylor unstable layer; they incorrectly attributed the first prediction to K. A. Smith [J. Fluid Mech. **24**, 401 (1966)]. Stable localized deformations have been predicted by R. J. Deissler and A. Oron [Phys. Rev. Lett. **68**, 2948 (1992)].

[5] For silicone oil (Dow Corning 200) and air, respectively, at 25 °C: $\rho = 0.969^a$, 0.00118^b g/cm^3; $\nu = 2.0^a$, 0.1568^b cm^2/s $\alpha = 0.00096^a$, 0.00339^b K^{-1}; $k = 15500^a$, 2650^b erg/(cm s K); $C_P = 1.469^a$, $1.005^c \times [10^7$ erg/(g K)]; $\kappa \equiv \frac{k}{\rho C_P} = 0.001088$, 0.2235 cm^2/s. The surface tension is $\sigma = 21.0^a$ dyn/cm and $\sigma_T = 0.068^d$ dyn/(cm K). These values are obtained from (a) Dow Corning 200 Silicone Oils data sheet; (b) *Properties of Materials at Low Temperature,* Natl. Bur. Stand. (U.S.) (Pergamon Press, New York, 1959); (c) H. J. Palmer and J. C. Berg, J. Fluid Mech. **47**, 779 (1971); (d) D. J. Poferl and R. Svehla, NASA Technical Note D-7488 (unpublished).

[6] S. J. VanHook, M. F. Schatz, J. B. Swift, W. D. McCormick, and H. L. Swinney, J. Fluid Mech. **345**, 45 (1997).

[7] M involves the temperature difference ΔT controlled in the experiment rather than the temperature difference across the liquid layer, which is given by (assuming conductive heat transfer) $\Delta T_{\text{liq}} = \Delta T(1 + d_g k/dk_g)^{-1}$.

[8] M. Fermigier, L. Limat, J. E. Wesfreid, P. Boudinet, and C. Quilliet, J. Fluid Mech. **236**, 349 (1992).

[9] A correction for finite cell size, $1 - [2\pi d/(q_{\text{cap}} L)]^2$, gives only a 3% reduction from (2).

[10] R. Becerril, S. J. VanHook, and J. B. Swift, Phys. Fluids **10**, 3230 (1998).